Songklanakarin J. Sci. Technol.
43 (6), 1597-1603, Nov. - Dec. 2021

http://www.sjst.psu.ac.th

Original Article

Identification of highly potent α-glucosidase inhibitors from *Garcinia schomburgkiana* and molecular docking studies

Thi My Lien Do[1], Nguyen-Minh-An Tran[2], Thuc-Huy Duong[3], Preecha Phuwapraisirisan[4], Nakorn Niamnont[5], Suttira Sedlak[6], Kewalin Inthanon[7], and Jirapast Sichaem[7*]

[1] *Institute of Environment-Energy Technology, Sai Gon University, Ho Chi Minh City, 748355 Vietnam*

[2] *Industrial University of Ho Chi Minh, Ho Chi Minh City, 748355 Vietnam*

[3] *Department of Chemistry, Ho Chi Minh University of Education, Ho Chi Minh City, 748355 Vietnam*

[4] *Center of Excellence in Natural Products Chemistry, Department of Chemistry, Faculty of Science, Chulalongkorn University, Pathum Wan, Bangkok, 10330 Thailand*

[5] *Organic Synthesis, Electrochemistry and Natural Product Research Unit, Department of Chemistry, Faculty of Science, King Mongkut's University of Technology Thonburi, Bangkok, 10140 Thailand*

[6] *Biodiversity and Conversation Research Unit, Walai Rukhavej Botanical Research Institute, Mahasarakham University, 44150 Thailand*

[7] *Research Unit in Natural Products Chemistry and Bioactivities, Faculty of Science and Technology, Thammasat University, Lampang Campus, Lampang, 52190 Thailand*

Received: 27 August 2020; Revised: 25 December 2020; Accepted: 28 December 2020

Abstract

Twenty-two compounds (**1-22**) were isolated from the stems and twigs of *Garcinia schomburgkiana*. NMR, IR, UV, and MS were used for structural elucidation, and comparisons were made with previous reports. Compound **1** exhibited the most potent α-glucosidase inhibition (IC_{50} 0.31 ± 0.7 μM), outperforming the positive control (acarbose). Molecular docking results showed that the phenolic hydroxyl groups on the phenyl rings linked with active receptor sites on the protein in **1**. By preventing the duplication of DNA sequences, Compound **1** is an excellent inhibitor of the α-glucosidase enzyme, and represents a potential novel class of α-glucosidase inhibitor.

Keywords: Clusiaceae, *Garcinia schomburgkiana*, α-glucosidase inhibition, molecular docking calculation

1. Introduction

Garcinia schomburgakiana Pierre (Clusiaceae), known in Thai as Ma-dan, is an edible evergreen tree that grows in Laos, Vietnam, Cambodia, and Thailand. It has ethnomedical uses as a laxative and expectorant, and in the treatment of coughs, menstrual disturbances, and diabetes (Mungmee, Sitthigool, Buakeaw, & Suttisri, 2013). Previous studies of the bioactive constituents of *G. schomburgkiana* have reported the presence of flavonoids, xanthones, triterpenoids, depsidones, phloroglucinols, and biphenyl derivatives, some of which exhibited antimalarial,

*Corresponding author
Email address: jirapast@tu.ac.th

cytotoxic, and anti *α*-glucosidase properties (Kaennakam, Mudsing, Rassamee, Siripong, & Tip-pyang, 2019; Le, Nishimura, Takenaka, Mizushina, & Tanahashi, 2016; Lien *et al.*, 2020; Sukandar, Siripong, Khumkratok, & Tip-Pyang, 2016).

In Thailand, *G. schomburgkiana* has been traditionally used for the treatment of diabetes (Meechai, Phupong, Chunglok, & Meepowpan, 2018). The goal of the present study was to identify any active *α*-glucosidase inhibitors. We isolated twenty-two compounds (**1**-**22**), including two bixanthones (**1** and **2**), seven xanthones (**3**-**9**), one biphenyl derivative (**10**), one lignin (**11**), one bifuraldehyde derivative (**12**), two flavonoids (**13** and **14**), two phloroglucinols (**15** and **16**), and six biflavonoids (**17**-**22**) from the *G. schomburgkiana* stems and twigs (Figure 1). The isolated compounds were evaluated for *α*-glucosidase inhibition, and molecular docking studies were performed to elucidate the mechanisms of inhibition.

2. Materials and Methods

2.1 Experimental procedures

The ^{1}H and ^{13}C NMR spectra were measured on a Bruker AVANCE 400 spectrometer. TLC was performed on precoated Merck silica gel 60 F_{254} plates (0.25 mm thickness). Spots were visualized under UV irradiation and heating after spraying with 10% (v/v) anisaldehyde. Organic solvents were distilled prior to use. Acarbose was supplied by Bayer Vitol Leverkusen, Germany. *α*-Glucosidase (EC 3.2.1.20) from *Saccharomyces cerevisiae* and 4-nitrophenyl-*α*-D-gluco pyranoside (*p*-NPG) were purchased from Sigma-Aldrich.

2.2 Plant material

Stems and twigs of *G. schomburgkiana* were collected on April 15, 2018 from Mueang Maha Sarakham District, Mahasarakham Province, Thailand (16.0132 °N, 103.1615 °E). Identification was confirmed by S. Sedlak, Walai Rukhavej Botanical Research Institute, Mahasarakham University, Thailand. A voucher specimen Khumkratok no. 92-08 was deposited at the Walai Rukhavej Botanical Research Institute, Mahasarakham University, Thailand.

2.3 Extraction and isolation

The stems and twigs (20.0 kg) were air-dried, and the powder was exhaustively extracted using 95% (v/v) EtOH (4 × 35 L) at room temperature. The filtered solution was concentrated to dryness (1.02 kg), and the crude extract was partitioned with H_2O and EtOAc to yield EtOAc extract (560.2 g). This extract was subjected to silica gel column chromatography (CC) and eluted with *n*-hexane:EtOAc (9:1-0:10) and EtOAc:MeOH (10:0-0:10) gradients, yielding fractions EA.1-EA.19. Fraction EA5 (1.6 g) was loaded into a silica gel CC (*n*-hexane:EtOAc (8:2)), yielding subfraction EA5.1-EA.5.5. Subfraction EA5.2 (0.6 g) was purified by CC (Sephadex LH-20), using CH_2Cl_2:MeOH (1:1) as eluent to afford **12** (1.4 mg). Subfraction EA5.3 (0.8 g) was separated in the same way but with further RP-C18 silica gel CC, then eluted with H_2O:MeOH (6:1) to give **11** (14.5 mg).

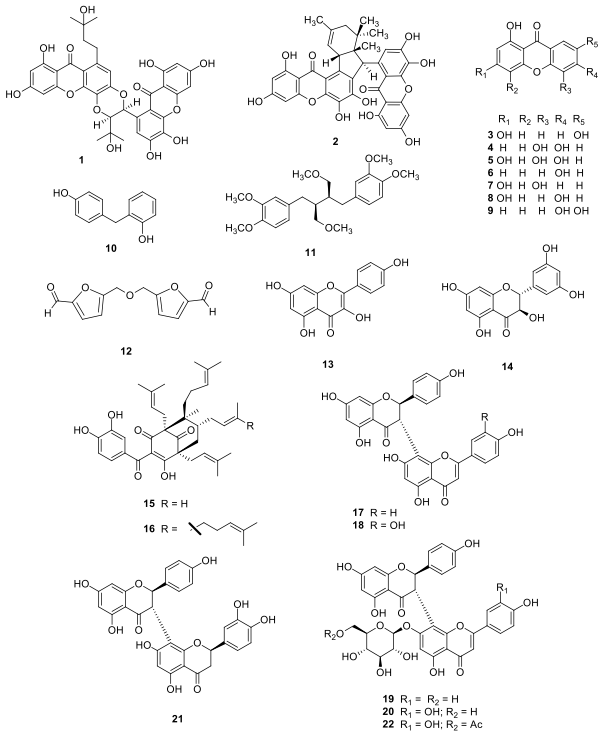

Figure 1. Chemical structures of **1**-**22**

Fraction EA6 (2.0 g) was separated by silica gel CC elution with *n*-hexane:EtOAc (8:2), yielding subfractions EA6.1–EA.6.6. Subfraction E4.7 (0.3 g) was isolated by Sephadex LH-20 CC with CH_2Cl_2:MeOH (1:1) and rechromatographed with RP-C18 silica gel CC using H_2O:MeOH (6:1) as eluent to give **10** (4.5 mg) and **13** (6.4 mg). Subfraction EA6.3 (0.8 g) was loaded into a silica CC, eluted with *n*-hexane-EtOAc (8:2), then purified (Sephadex LH-20 CC, CH_2Cl_2:MeOH (1:1) as eluent) and reisolated with RP-C18 silica gel CC eluted with H_2O:MeOH (6:4) to yield 3 (21.5 mg) and **4** (10.0 mg). Fraction EA7 (3.7 g) was separated in the same way, giving subfractions EA7.1-EA.7.6. Subfraction EA7.2 (0.5 g) was purified by CC (Sephadex LH-20, CH_2Cl_2:MeOH (1:1) as eluent) followed by RP-C18 silica gel CC (H_2O-MeOH (5:1)) to give **2** (11.5 mg), **5** (12.4 mg), and **6** (2.4 mg). Subfraction EA7.3 (0.8 g) was subjected to silica gel CC, eluted with *n*-hexane:EtOAc (8:2), purified using the Sephadex LH-20 CC (100 g) with CH_2Cl_2:MeOH (1:1) as gradient, then subjected to RP-C18 silica gel CC (H_2O:MeOH (5:1)) to afford **7** (25.0 mg) and **8** (20.0 mg).

Fraction EA9 (10.5 mg) was loaded into a silica gel CC using n-hexane:EtOAc (8:2) as eluent to yield 1 (20.3 mg), 9 (2.0 mg), **14** (2.2 mg), **16** (2.4 mg), and **15** (1.2 mg). Fraction EA11 (45.0 g) was passed through Sephadex LH-20 CC with CH_2Cl_2:MeOH (1:1), yielding subfractions EA11.1-EA11.4. Subfraction EA11.2 (60.0 mg) was purified using silica gel CC with n-hexane:EtOAc (7:3) as eluent to yield 13 (1.2 mg), **14** (1.7 mg), and **15** (1.4 mg). Subfraction EA11.4 (75.0 mg) was separated in a silica gel CC eluted with n-hexane:EtOAc (6:4) to give **16** (3.2 mg) and **17** (1.5 mg). Fraction EA13 (25.5 mg) was separated in a similar manner to fraction EA11 to give **18** (2.1 mg) and **19** (2.4 mg). Fraction EA13 (25.5 mg)

was passed through Sephadex LH-20 CC with CH_2Cl_2:MeOH (1:1) then purified by silica gel CC (6:4 n-hexane:EtOAc) to yield **20** (1.1 mg), **21** (1.9 mg), and **22** (1.0 mg).

2.4 α-Glucosidase inhibition assay

Test compounds were evaluated for inhibitory activity against baker's yeast α-glucosidase, following the previous protocol (Sichaem, Aree, Lugsanangarm, & Tip-pyang, 2017) with small modification. A 10 µL sample was incubated with 0.1 U/mL α-glucosidase solution in 1 mM phosphate buffer (pH 6.9) for 10 min at 37 °C. The reaction was initiated by the addition of 50 µL of 1 mM *p*-nitrophenyl-α-D-glucopyranoside (*p*-NPG) followed by incubation for a further 20 min. The reaction was terminated by adding 100 µL of 1 M Na_2CO_3. The reaction was quantified using a UV microplate reader (405 nm). Acarbose was used as a standard reference drug and enzyme activity was calculated as follows:

$$\frac{(A_0 - A_1)}{A_0} \times 100$$

where A_1 and A_0 are absorbances with and without the sample, respectively

The determination of kinetic parameters of the most active compound against α-glucosidase was performed according to our previous method (Sichaem *et al.*, 2017).

2.5 Molecular docking calculation

Compound **1** had the strongest α-glucosidase inhibition, and was therefore selected for the molecular docking studies. These were performed using glycosidase human amylase (5KEZ:PDB, at a resolution of 1.83 Å from PDB: 10.2210/pdb5KEZ/pdb). AutoDockTools package was conducted for docking of the receptor and ligand. The target protein or a receptor was performed to delete small molecules like water, small ligands, and heteroatoms and saved in *.pdb format files using the Discovery Studio 2019 Client (DSC) package (Sudileti *et al.*, 2019). The ligands (**1** and acarbose) were optimized by the Avogadro package *via* the MMFF94 method. The minimum energy of ligand conformation was picked (Hanwell *et al.*, 2012). The AutoDock package fully predicts the minimum negative free energy binding (ΔG) of a receptor and ligand reaction system and the inhibition constant, K_i (IC_{50} *in silico* docking). For the receptor, the polar hydrogen and Kollman charges were added to all atoms and files were saved in pdbqt format (receptor.pdbqt). For the ligand all polar hydrogens were added, Gasteiger charges were computed, non-polar hydrogen was merged, and files were saved in pdbqt format (ligand.pdbqt). The grid file (dock.gpf) parameters were set as grid point spacing. The number of user-specified grid points and coordinates of the central grid points of maps had values of 0.375Å, (120 × 120 × 120) and (X = -38.324, Y=10.387, Z= 94.100). The parameters in the docking file (dock.dpf) were set at run times of 100 after 2500000 energy evaluations. A conformation ligand (**1** or acarbose) was assumed to dock to a receptor (5KEZ) based on a Lamarckian genetic model. Calculation results were saved in a logic dock file (dock.dlg) (Thiratmatrakul *et al.*, 2014). The Discovery Studio and Molegro (MMV) packages were conducted to visualize and present the results. The ATD can be run directly by command menu or by DOS commands from system prompt C:>by typing autogrid4.exe -p dock.gpf -l dock.glg & or autodock4.exe -p dock.dpf -l dock.dlg, respectively.

3. Results and Discussion

The dried *G. schomburgkiana* stems and twigs were extracted using EtOH. This crude extract was fractioned and purified using chromatographic techniques to furnish schomburgkixanthone (**1**) (Lien *et al.*, 2020), griffipavi xanthone (**2**) (Xu *et al.*, 1998), 1,3,7-trihydroxyxanthone (**3**) (Meechai, *et al.*, 2016), 1,5,6-trihydroxyxanthone (**4**) (Wu, Wang, Du, Yang, & Xiao, 1998), 1,3,5,6-tetrahydroxy xanthone (**5**) (Sia, Bennett, Harrison, & Sim, 1995), 1,6-dihydroxyxanthone (**6**) (Madan *et al.*, 2002), 1,3,5-trihydroxyxanthone (**7**) (Kitanov & Nedialkov, 2001), 1,3,6-trihydroxyxanthone (**8**) (Chan, 2013), 1,6,7-trihydroxy xanthone (**9**) (Fu *et al.*, 2015), 2,4′-dihydroxydiphenylmethane (**10**) (Fisher, Chao, Upton, & Day, 2002), phyllanthin (**11**) (Nguyen *et al.*, 2013), 5,5′-[oxybis(methylene)]di(2-furaldehyde) (**12**) (Amarasekara, Nguyen, Du, & Kommala pati, 2019), kaempferol (**13**) (Xiao *et al.*, 2006), 5,7,3′,5′-tetrahydroxyflavanonol (**14**) (Zhang *et al.*, 2007), guttiferone K (**15**) (Cao *et al.*, 2007), oblongifolin C (**16**) (Hamed *et al.*, 2006), volkensiflavone (**17**), morelloflavone (**18**), volkensi flavone-7-*O*-glucopyranoside (**19**), morelloflavone-7-*O*-glucopyranoside (**20**) (Jamila, Khan, Khan, Khan, & Khan, 2016), fukugetin (**21**) (Compagnone, Suarez, Leitao, & Delle Monache, 2008), and (2*S*,3*S*)-morelloflavone-7-*O*-β-acetylglucopyranoside (**22**) (Mountessou *et al.*, 2018). These were identified by comparing their NMR spectra with published data (Figure 1).

Isolated compounds **1**-**11**, **13**-**19**, and **21** were tested for α-glucosidase inhibitory activity (Table 1). Compounds **1**, **2**, **4**, **5**, **9**, and **14**-**19** exhibited potent inhibition of α-glucosidase with the IC_{50} values were in the range of 0.31 ± 0.7 to 97.8 ± 0.2 µM, greater than the standard, acarbose (IC_{50} 147 ± 0.5 µM). From above results, compound **1** revealed the highest potential inhibitory activity against α-glucosidase. Thus, it was necessary to study type of α-glucosidase inhibition of **1**. Lineweaver-Burk plots were drawn by measuring three different *p*-NPG concentrations (0.29, 0.012, and 9.29×10^{-5} mM); all of which intersected at the second quadrant. The kinetic analysis indicated that V_{max} decreased with the increasing concentrations of **1** while K_m increased. This behavior suggested that compound **1** inhibited yeast α-glucosidase in a mixed-type manner.

Compound **1** showed the strongest *in vitro* inhibition among the active compounds, with an IC_{50} value of 0.31 ± 0.7 µM. As shown in Figure 2, the most stable ligand (**1**) was immersed in a receptor 5KEZ after completion of docking. It bonded to the active sites of the 5KEZ receptor with free energy bonding (ΔG) of -8.86 kcal.mol^{-1} and an inhibition constant K_i of 0.323 µM. In comparison, the *in silico* values for acarbose were -4.10 kcal.mol^{-1} and 989 µM, respectively. The maximum negative conformation of **1** indicated that bonding between the ligand and the active sites of the receptor was more stable than binding of acarbose to the same receptor. The greater stability of bonding between **1** and the receptor was apparent from the lower free energy binding value. The IC_{50} *in vitro* value and *in silico* inhibition constant K_i of **1** confirmed it to be a stronger inhibitor than acarbose in both *in vitro and in silico* molecular docking. As

Table 1. α-Glucosidase inhibition (IC_{50} ± SD) of isolated compounds

Compound	IC_{50} (μM)
1	0.31 ± 0.7
2	11.8 ± 0.1
3	NI[a]
4	92.5 ± 1.5
5	97.8 ± 0.2
6	NI[a]
7	NI[a]
8	NI[a]
9	73.7 ± 0.2
10	NI[a]
11	NI[a]
12	NT[b]
13	NI[a]
14	62.9 ± 0.1
15	12.1 ± 1.6
16	10.6 ± 2.4
17	28.9 ± 0.1
18	25.6 ± 0.5
19	14.3 ± 2.3
20	NT[b]
21	NI[a]
22	NT[b]
Acarbose	147 ± 0.5

[a] No inhibition (inhibitory effect less than 30% at concentration of 1 mg/mL). [b] Not tested

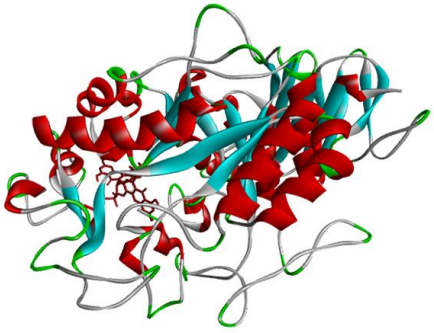

Figure 2. Conformation of (**1**) docked with a receptor 5KEZ:PDB for inhibition of glycosidase human amylase and classified as a hydrolase inhibitor, after completion of calculated docking. The lowest negative free energy of binding of -8.86 kcal.mol^{-1} and an inhibition constant of 0.323 μM

shown in Figures 4-5 and Table 2, in its most stable conformation, **1** formed eight hydrogen bonding from the oxygen and hydrogen atoms on the active sites of the ligand to the residual amino acids of a receptor 5KEZ, including Asn152 Ile235, His305, Asp300, and Gly239. The phenolic hydroxyl groups on the aromatic rings at C-1, C-3, and C-3′ were the indicated sites on the conformation ligand where hydrogen bonds formed with the amino acids. This established that the phenolic hydroxyl groups on the phenyl rings linked to active receptor sites on the protein in **1**, preventing duplication of the DNA sequences. This made compound **1** an excellent inhibitor of the α-glucosidase enzyme. As shown in Figures 3 and 5, the residual amino acids were those of the A: chain- Asn152, Gly306, Gln239, Glu240, Leu237, His305, Asp300, Ala198, Val234, Ile235, Lys200, Tyr151, and those

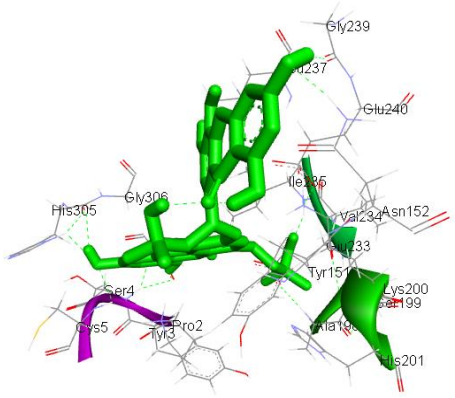

Figure 3. Residual amino acids of receptor 5KEZ forming hydrogen bonds with active sites of ligand (**1**)

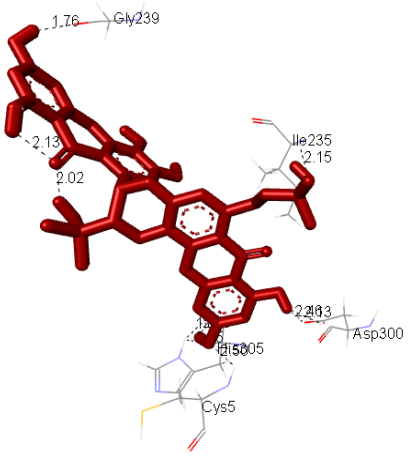

Figure 4. Hydrogen bonding of the residual amino acids of receptor (**1**) with the most stable ligand were 8 hydrogen bonds

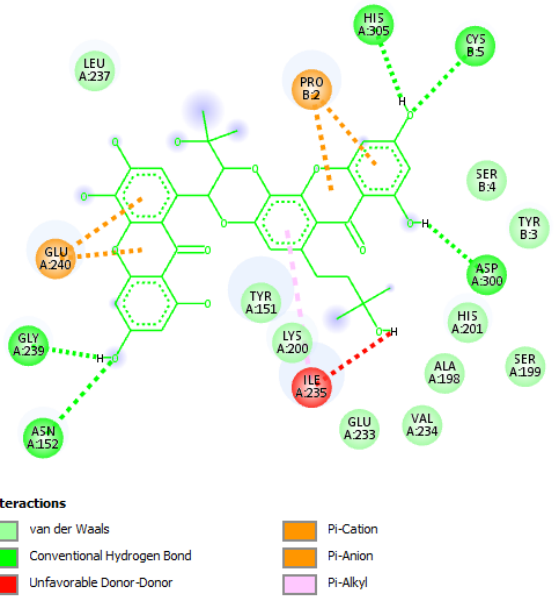

Figure 5. Interactions between amino acid of receptor and ligand **1** shown as 2D diagram with hydrogen bonds, Van der Waals force, unfavorable donor-donor, pi-cation, pi-anion, and pi-alkyl interactions

Table 2. Significant results for the docking of **1** and acarbose to active sites on glycosidase human amylase (5KEZ: PDB) receptor

Entry	Free Energy of Binding[a]	K_i[b]	Number of hydrogen bonds[c]	Property and bond length[d]
1	-8.86	0.323	8	A:Asn152:H - **1**:O (2.19) A:Ile235:H - **1**:O (2.15) A:His305:H - **1**:O (2.46) B:Cys5:H - **1**:O (2.50) **1**:H - A:His305:O (2.40) **1**:H - A:Asp300:O1 (2.46) **1**:H - A:Asp300:O2 (2.13) **1**:H - A:Gly239:O (1.76)
Acarbose	-4.10	989	11	A:Ser3:O - Acarbose: O (2.59) A:Thr6:O - Acarbose: O (3.16) A:SER226:O - Acarbose:O (3.12) Acarbose: H - A:Asp402:O (1.75) Acarbose: H - A:Asp402:O (2.07) Acarbose: H - A:Asp402:O (1.85) Acarbose: H - A:Asp402:O (2.33) Acarbose: H - A: Asn5:O (2.08) Acarbose: H - A:Asn5:O (2.04) Acarbose: H - A:Ser3:O (2.25) Acarbose: H - A:Arg10:O (2.27)

[a] In units of kcal.mol^{-1} from the Auto Dock Tools (ATD) package. [b] Inhibition constant in units of µM and calculated by ATD. [c] From the Discovery Studio (DSC) package after completion of calculated docking. [d] Calculated by the ATD package and visualized by the DSC package in angstroms

of the B: chain: Pro2, Cys5, Ser4, and Tyr3. When divided by hydrophobicity and hydrophilicity, the hydrophobic amino acids of the A and B chain were Leu237, Ala198, Val234, Ile235, and Cys5. The remaining amino acids were Asn152, Gly239, Glu240, His305, Asp300, His201, Ser199, Glu233, Lys200, Tyr151, Gly306, Tyr3, Pro2, and Ser4. As shown in Figure 7, the active sites of ligand **1** formed hydrogen bonds with residual amino acids on the A and B chains: Asp300 (hydrophilic), His305 (hydrophilic), Gly239 (hydrophilic), Asn152 (hydrophilic), and Cys5 (hydrophobic). The remaining links from ligand to receptors were due to the Van der Waals force, unfavorable donor-donor, pi-cation, pi-anion, and pi-alkyl. Together, these determined the free energy bonding and inhibition constant in the most stable conformation. The ligand map identified secondary interactions including hydrogen bonding, steric, and overlap, which were implicated in the most stable interaction between **1** and a receptor 5KEZ. The green lines exposed the steric effects, which determined the conformation of the molecular binding process. The size of the pink circles in Figure 6 reflects the strength of overlap interactions and contribution to steric hindrance. The hydrophobicity of the most stable conformation is identified by the frontier in Figure 7.

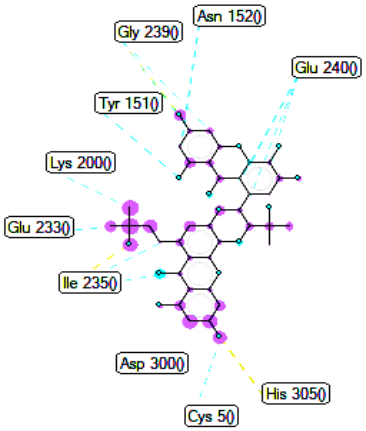

Figure 6. Ligand map showing secondary interactions including hydrogen bonds, steric, and overlap

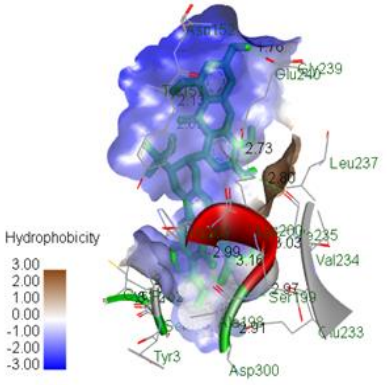

Figure 7. Frontier of the most stable conformation of **1** showing hydrophobicity of conformation

4. Conclusions

In this study, twenty-two natural compounds (**1**-**22**) were isolated from stems and twigs of *G. schomburgkiana*. Compound **1** exhibited the strongest activity against *α*-glucosidase, outperforming acarbose, a positive control. In the molecular docking model, the phenolic hydroxyl groups of **1** on the aromatic ring at C-1, C-3, and C-3′ formed active sites on the ligand, and these formed hydrogen bonds with the residual amino acids of the receptor. The study established that linking of the phenolic hydroxyl groups on the phenyl rings to active sites on proteins in **1** prevented duplication of

DNA sequences. This makes compound **1** an excellent inhibitor of the α-glucosidase enzyme.

Acknowledgements

This work was supported by Thammasat University Research Unit in Natural Products Chemistry and Bioactivities and by the Thailand Research Fund (TRF) (Grant No. MRG6180104).

References

Amarasekara, A. S., Nguyen, L. H., Du, H., & Kommalapati, R. R. (2019). Kinetics and mechanism of the solid-acid catalyzed one-pot conversion of D-fructose to 5, 5′-[oxybis (methylene)] bis [2-furaldehyde] in dimethyl sulfoxide. *SN Applied Sciences*, *1*(9), 964. doi:10.1007/s42452-019-0994-2

Cao, S., Brodie, P. J., Miller, J. S., Ratovoson, F., Birkinshaw, C., Randrianasolo, S., . . . Kingston, D. G. (2007). Guttiferones K and L, antiproliferative compounds of *Rheedia calcicola* from the Madagascar rain forest. *Journal of Natural Products*, *70*(4), 686-688. doi:10.1021/np070004i

Chan, S. L. (2013). *Synthesis and antioxidant activity of Prenylated Xanthones derived from 1, 3, 6-Trihydroxyxanthone* (Doctoral thesis, Universiti Tunku Abdul Rahman, Negeri Perak, Malaysia). Retrieved from http://eprints.utar.edu.my/892/1/CE-2013-0903483.pdf

Compagnone, R. S., Suarez, A. C., Leitao, S. G., & Delle Monache, F. (2008). Flavonoids, benzophenones and a new euphane derivative from *Clusia columnaris* Engl. *Revista Brasileira de Farma cognosia*, *18*(1), 6-10. doi:10.1590/S0102-695X2008000100003

Fisher, T. H., Chao, P., Upton, C. G., & Day, A. J. (2002). A 13C NMR study of the methylol derivatives of 2, 4′-and 4, 4′-dihydroxydiphenylmethanes found in resol phenol–formaldehyde resins. *Magnetic Resonance in Chemistry*, *40*(11), 747-751. doi:10.1002/mrc.1089

Fu, W.M., Tang, L.P., Zhu, X., Lu, Y.F., Zhang, Y.L., Lee, W.Y.W., Wang, H., Yu, Y., Liang, W.C., Ko, C.H., & Xu, H. X. (2015). MiR-218-targeting-Bmi-1 mediates the suppressive effect of 1,6,7-trihydroxyxanthone on liver cancer cells. *Apoptosis*, *20*(1), 75-82. doi:10.1007/s10495-014-1047-3

Hamed, W., Brajeul, S., Mahuteau-Betzer, F., Thoison, O., Mons, S., Delpech, B., Hung, N.V., Sévenet, T., & Marazano, C. (2006). Oblongifolins A-D, polyprenylated benzoylphloroglucinol derivatives from *Garcinia oblongifolia*. *Journal of Natural Products*, *69*(5), 774-777. doi:10.1021/np050543s

Hanwell, M. D., Curtis, D. E., Lonie, D. C., Vandermeersch, T., Zurek, E., & Hutchison, G. R. (2012). Avogadro: an advanced semantic chemical editor, visualization, and analysis platform. *Journal of Cheminformatics*, *4*(1), 17. doi:10.1186/1758-2946-4-17

Jamila, N., Khan, N., Khan, I., Khan, A. A., & Khan, S. N. (2016). A bioactive cycloartane triterpene from *Garcinia hombroniana*. *Natural Product Research*, *30*(12), 1388-1397. doi:10.1002/mrc.4071

Kaennakam, S., Mudsing, K., Rassamee, K., Siripong, P., & Tip-pyang, S. (2019). Two new xanthones and cytotoxicity from the bark of *Garcinia schomburgkiana*. *Journal of Natural Medicines*, *73*(1), 257-261. doi:/1007.10s8-1240-018-11418

Kitanov, G. M., & Nedialkov, P. T. (2001). Benzophenone *O*-glucoside, a biogenic precursor of 1,3,7-trioxygenated xanthones in *Hypericum annulatum*. *Phytochemistry*, *57*(8), 1237-1243. doi:10.1016/S0031-9422(01)00194-7

Le, D. H., Nishimura, K., Takenaka, Y., Mizushina, Y., & Tanahashi, T. (2016). Polyprenylated benzoylphloro glucinols with DNA polymerase inhibitory activity from the fruits of *Garcinia schomburgkiana*. *Journal of Natural Products*, *79*(7), 1798-1807. doi:10.1021/acs.jnatprod.6b00255

Lien Do, T. M., Duong, T. H., Nguyen, V. K., Phuwaprai sirisan, P., Doungwichitrkul, T., Niamnont, N., Jarupinthusophon S., & Sichaem, J. (2020). Schomburgkixanthone, a novel bixanthone from the twigs of *Garcinia schomburgkiana*. *Natural Product Research*, 1-6. doi:10.1080/14786419.2020.1716351

Madan, B., Singh, I., Kumar, A., Prasad, A. K., Raj, H. G., Parmar, V. S., & Ghosh, B. (2002). Xanthones as inhibitors of microsomal lipid peroxidation and TNF-α induced ICAM-1 expression on human umbilical vein endothelial cells (HUVECs). *Bioorganic & Medicinal Chemistry*, *10*(11), 3431-3436. doi: 10.1016/S0968-0896(02)00262-6

Meechai, I., Phupong, W., Chunglok, W., & Meepowpan, P. (2016). Anti-radical activities of xanthones and flavonoids from *Garcinia schomburgkiana*. Retrieved from http://cmuir.cmu.ac.th/jspui/handle/6653943832/56293

Meechai, I., Phupong, W., Chunglok, W., & Meepowpan, P. (2018). Dihydroosajaxanthone: a new natural xanthone from the branches of *Garcinia schomburgkiana* Pierre. *Iranian Journal of Pharmaceutical Research*: IJPR, 17(4), 1347. doi:10.22037/IJPR.2018.2292

Mountessou, B.Y.G., Tchamgoue, J., Dzoyem, J.P., Tchuenguem, R.T., Surup, F., Choudhary, M.I., Green, I.R., & Kouam, S. F. (2018). Two xanthones and two rotameric (3⟶ 8) biflavonoids from the Cameroonian medicinal plant *Allanblackia floribunda* Oliv. (Guttiferae). *Tetrahedron Letters*, *59*(52), 4545-4550. doi:10.1016/j.tetlet.2018.11.035

Mungmee, C., Sitthigool, S., Buakeaw, A., & Suttisri, R. (2013). A new biphenyl and other constituents from the wood of *Garcinia schomburgkiana*. *Natural Product Research*, *27*(21), 1949-1955. doi:10.1080/14786419.2013.796469

Nguyen, D. H., Sinchaipanid, N., & Mitrevej, A. (2013). *In vitro* intestinal transport of phyllanthin across Caco-2 cell monolayers. *Journal of Drug Delivery Science and Technology*, *23*(3), 207-214. doi:10.1016/S1773-2247(13)50032-3

Sia, G. L., Bennett, G. J., Harrison, L. J., & Sim, K. Y. (1995). Minor xanthones from the bark of *Cratoxylum cochinchinense*. *Phytochemistry*, *38*(6), 1521-1528.

doi:10.1016/0031-9422(94)00526-Y

Sichaem, J., Aree, T., Lugsanangarm, K., & Tip-pyang, S. (2017). Identification of highly potent α-glucosidase inhibitory and antioxidant constituents from *Zizyphus rugosa* bark: enzyme kinetic and molecular docking studies with active metabolites. *Pharmaceutical Biology*, *55*(1), 1436-1441. doi:10.1080/13880209.2017.1304426

Sudileti, M., Nagaripati, S., Gundluru, M., Chintha, V., Aita, S., Wudayagiri, R., Chamarthi, N., & Cirandur, S. R. (2019). rGO-SO3H Catalysed green synthesis of fluoro-substituted aminomethylene bisphosphonates and their anticancer, molecular docking studies. *Chemistry Select*, *4*(44), 13006-13011. doi:10.1002/slct.201903191

Sukandar, E. R., Siripong, P., Khumkratok, S., & Tip-pyang, S. (2016). New depsidones and xanthone from the roots of *Garcinia schomburgkiana. Fitoterapia*, *111*, 73-77. doi: 10.1016/j.fitote.2016.04.012

Thiratmatrakul, S., Yenjai, C., Waiwut, P., Vajragupta, O., Reubroycharoen, P., Tohda, M., & Boonyarat, C. (2014). Synthesis, biological evaluation and molecular modeling study of novel tacrine–carbazole hybrids as potential multifunctional agents for the treatment of Alzheimer's disease. *European Journal of Medicinal Chemistry*, *75*, 21-30. doi:10.1016/j.ejmech.2014.01.020

Wu, Q. L., Wang, S. P., Du, L. J., Yang, J. S., & Xiao, P. G. (1998). Xanthones from *Hypericum japonicum* and *H. henryi*. *Phytochemistry*, *49*(5), 1395-1402. doi: 10.1016/S0031-9422(98)00116-2

Xiao, Z. P., Wu, H. K., Wu, T., Shi, H., Hang, B., & Aisa, H. A. (2006). Kaempferol and quercetin flavonoids from *Rosa rugosa. Chemistry of Natural Compounds*, *6*(42), 736-737. doi: 10.1007/s10600-006-0267-3

Xu, Y.J., Cao, S.G., Wu, X.H., Lai, Y.H., Tan, B.H.K., Pereira, J.T., Goh, S.H., Venkatraman, G., Harrison, L.J., & Sim, K. Y. (1998). Griffipavixanthone, a novel cytotoxic bixanthone from *Garcinia griffithii* and *G. pavifolia. Tetrahedron Letters*, *39*(49), 9103-9106. doi:10.1016/S0040-4039(98)02007-3

Zhang, Y., Que, S., Yang, X., Wang, B., Qiao, L., & Zhao, Y. (2007). Isolation and identification of metabolites from dihydromyricetin. *Magnetic Resonance in Chemistry*, *45*(11), 909-916. doi:10.1002/mrc.2051